ISSN : 0974 - 7494 Volume 9 Issue 4

Nano Science and Nano Technology
An Indian Journal

Full Paper

NSNTAIJ, 9(4), 2015 [123-130]

Preparation $CuInSe_2$ (CIS) by arrested precipitation method as alight absorption layer of photovoltaic solar-cells

Wasan R.Saleh, Omar A.Ali*
Department of Physics, College of Science, University of Baghdad, Baghdad, (IRAQ)
E-mail: omarlibra2005@yahoo.com

ABSTRACT

The $CuInSe_2$ (CIS) nanocrystals are synthesized by arrested precipitation from molecular precursors are added to a hot solvent with organic capping ligands to control nanocrystal formation and growth.CIS thin films deposited onto glass substrate by spray – coating, then selenized in Ar-atmosphere to form CIS thin films.PVs were made with power conversion efficiencies of 0.631% as –deposited and 0.846% after selenization, for Mo coated, under AM 1.5 illumination. X-ray diffraction (XRD) and energy dispersive spectroscopy (EDS) analysis it is evident that CIS have the chalcopyrite structure as the major phase with a preferred orientation along (112) direction and the atomic ratio of Cu : In : Se in the nanocrystals is nearly 1 : 1 : 2.

KEYWORDS

$CuInSe_2$;
Nanoink;
Arrested precipitation;
Selenization:
Ar- Atmosphere.

INTRODUCTION

Chalcopyrite semiconductors such as $CuInSe_2$ (CIS) and and $Cu(In,Ga)Se_2$ (CIGS)are becoming popular as alight absorption layer of photovoltaic solar-cells (PVSCs).The previously and presently used $PVSC_s$ material, such as Si, is not ideal because of its low conversion efficiency and high production cost. Therefore, chalcopyrite semiconductor like CIS, which has high conversion efficiency and low cost, is expected to be $PVSC_s$ materials for next generation. CIS has a direct band gap suitable for the absorption of sunlight and a large light absorption coefficient, therefore, CIS can be used as thin film. Moreover, the processing of CIS is relatively easy due to its self-regeneration function[1,2].CIS is becoming one of the most promising materials for solar cell applications. CIS alloys have appropriate band gaps, reasonable work functions, high optical absorption coefficients, appropriate charge densities and mobilities to serve as PV absorber layers. Recently it is reported that CIS based solar cell achieved a remarkable efficiency of 18.8%[3]. Its band gap (1.04 eV) and good absorption coefficient (10^5 cm^{-1}) for solar spectrum make this material an excellent candidate for a solar cell absorber layer[4,5]. Various techniques are reported for the preparation of CIS films such as elemental co-evaporation[6], sputtering[7] and electro deposition[8]. However, it becomes necessary to produce device quality CIS films through a low-cost, eco-friendly and easily scalable process for mass production of films for PV applications. The most widely accepted methods are co-evaporation of the elements[6] and

Full Paper

annealing of Cu–In precursors in H_2Se/Se atmosphere[9,10]. Both processes involve Se vapor or H_2Se gas which are extremely toxic to health and environment.

In this work, The nanocrystals are synthesized by arrested precipitation from molecular precursors are added to a hot solvent with organic capping ligands to control nanocrystal formation and growth. Arrested precipitation has been a particularly effective way to obtain nanocrystals with a wide range of compositions, and tunable sizes and shapes[11,12]. Mo/CIS thin films deposited onto glass substrate by spray – coating and selenized in Ar-atmosphere to form CIS thin films.

EXPERIMENTS

Soda lime glass(SLG) (Delta Technologies, 25 mm × 25 mm × 1.1 mm polished float glass), Cr (99.999%, Lesker), Molybdenum (Mo) (Lesker 99.95%), ZnO target (Lesker, 99.9%) in a 0.5% O_2 in Ar atmosphere (Praxair, 99.95%) and ITO target (Lesker, 99.99% In_2O_3:SnO_2 90:10) in Ar atmosphere (Praxair, research grade)oleylamine (OLA; >70%), diphenylphosphine (DPP; 97%), copper(I) chloride (CuCl; 99.995+%), indium(III) chloride ($InCl_3$; anyhydrous 99.99%), elemental selenium (Se, 99.99%), cadmium sulfate ($CdSO_4$, 99.999%) from Aldrich Chemical Co.; Ammonium hydroxide (18 M NH_4OH), toluene, ethanol, were obtained from Fisher Scientific; and thiourea (99.999%) from Fluka Co.; Oleylamine was degassed by pulling vacuum overnight at ~200 mTorr at 110 °C and stored in an N_2 filled glovebox before use. All other chemicals were used as received without further purification. Copper (I) chloride, indium (III) chloride, DPP and degassed OLA were stored in a nitrogen-filled glovebox to prevent degradation.

CIS nanocrystals were synthesized using a modification of published procedures in[13-15] In a typical reaction, 2 mmol of CuCl, 2 mmol of $InCl_3$ and 13 mL of degassed oleylamine are added to a 100 mL three-neck flask after cleaningwhich input inside an N_2 filled glovebox (name solution 1). Reaction 4 mmol of Se, 2 mL of degassed oleylamine, and 1.5 mL of DPP added to vial of 25 mL (name solution 2) stirrer and heat into dissolve. The flask of sol. 1 is attached to a standard Schlenk line and degassed at 110 °C under a vacuum for 30 min. The flask is then filled with nitrogen and heated to 240 °C for 1 hr, and when the temperature reached to 180 °C injected the sol. 2 was injected, the color of solution changed to black immediately. The heating mantle is removed and the reaction is allowed to cool to the room temperature. The resulted nanocrystals are washed via centrifugation using toluene and ethanol. The contents of the reaction vessel and 10 mL of ethanol are mixed in a glass centrifuge tube and the nanocrystal product is precipitated by centrifugation at 6000 rpm for 3 min., so supernatant is discarded. The product nanocrystals is redispersed in 5 mL of toluene and centrifuged at 6000 rpm for 3 min. to remove the larger and poorly capped product. The supernatant is added to a new glass centrifuge tube and the precipitate is discarded. Ethanol is then slowly added to the nanocrystals dispersion until the mixture becomes slightly turbid. The mixture is centrifuged at 6000 rpm for 3 min. to again precipitate the nanocrystal product. The supernatant is discarded and the solid product is redispersed in toluene to a final concentration of 20 mg mL^{-1}. The final nanocrystals dispersion is then transferred to a glovebox for the ligand exchange.

Selenization of nanocrystal films took place inside a graphite cylinder, sealed and purged with pure Ar to achieve an inert atmosphere. The tube furnace was heated up to selenization temperature typically 525°C for 60 minutes, and then cooled down to the room temperature. The graphite cylinder was opened within an inert atmosphere glovebox and the films were removed and saved in the glovebox

For morphological structure studies, transmission electron microscopy (TEM) was performed using a JEOL 2010F TEM at 200 kV accelerating voltage. TEM samples were prepared by drop casting from chloroform onto a 200 mesh nickel grid with a carbon film (Electron Microscopy Sciences). Energy dispersive X-ray spectroscopy (EDS) was carried out using an Oxford INCA EDS detector on the JEOL 2010F TEM. Scanning electron microscopy (SEM) was performed on a Zeiss Supra 40 VP SEM operated at 5 keV accelerating voltage

through an In- lens detector with samples grounded using copper tape.

For structural study X-ray diffraction (XRD) was performed using a Rigaku R-Axis Spider diffractometer with an image-plate detector and Cu Kα (λ = 1.54 Å) radiation operated at 40 kV and 40 mA. XRD samples were prepared by drying a drop of concentrated nanoparticle dispersion onto a glass slide in a glovebox. The nanocrystal powder was then suspended on a 0.5 mm nylon loop using mineral oil for analysis. Samples were scanned for 15 min while rotating at 2°/s. The 2D diffraction patterns were integrated using the Rigaku 2DP powder processing suite with subtraction of the background scattering from the nylon loop and mineral oil.

Conductive back contacts Mowere deposited separately on sodalime glass after cleaned by sonication in an acetone/isoproponol mixture, followed by rinse with distilled water (DI) water, and drying under a nitrogen. Molybdenum of 500 nm thick was deposited by RF sputtered while the gold was thermally evaporated. 10 mg mL^{-1} solutions of nanoparticles were prepared for the spray-deposition. CIS nanocrystal layers were spray-coated with an airbrush (SONOTEK) operated at 1.6 psig of head pressure. A CdS buffer layer was deposited by chemical bath deposition following procedures described by McCandless and Shafarman[16]. Briefly, A CdS buffer layer was deposited by dropping 0.7 mL of a CdS precursor solution (1.25 mL of 15 mM $CdSO_4$, 2.2 mL of 1.5 M thiourea, and 2.8 mL of 18 M NH_4OH in water) onto the CIS nanocrystal film and heated to 95 °C on a hot plate and covered with an inverted crystallization dish for 2 min. The substrate was removed from the hot plate, rinsed with DI water, and dried with a stream of compressed air. Top layers of ZnO and ITO were deposited by RF sputtering from a 40 nm ZnO target and a 300 nm of ITO target. ZnO and ITO are deposited selectively onto 8 rectangular regions with active device areas of 0.08 cm^2 (8 mm^2 a 4mm x 2mm rectangle). Silver paint was applied for electrical contact to the devices.

PV device response was measured using a Keithley 2400 General Purpose Sourcemeter under solar simulation using a Newport Xenon Lamp Solar Simulator with an AM1.5 filter (100 mW/cm^2). Intensity of the light source was calibrated using a NIST calibrated Si photodiode (Hamamatsu, S1787-08). Different fractions of solar spectrum were generated by placing colored glass cutoff filters (Newport) directly in the path of light beam emanating from the solar simulator. Incident photon conversion efficiency (IPCE) was measured using a home-built device with lock-in amplifier (Stanford Research Systems, model SR830) and monochromator (Newport Cornerstone 260 1/4M). IPCE was calibrated with Si and Ge photodiodes (Hamamatsu).

RESULTS AND DISCUSION

Figure 1 shows the atomic ratio of Cu : In : Se in the nanocrystals determined by EDS is nearly 1:1:2.

The nanocrystals disperse in various organic solvents, including chloroform, hexane, toluene and acetone. Toluene was used as the dispersing solvent for the nanocrystal inks which is used to fabricate devices, as it provided the most uniform coatings of the solvents that were tested. TABLE 1 summarizes the composition of CIS nanoink determined by EDS.

Figure 2 shows TEM images for the oleylamine capped CIS nanocrystals. The nanocrystals are composed of chalcopyrite CIS. TEM images of CIS nanocrystals shows the nanocrystals are irregularly shaped and rather polydisperse.

Figure 3A shows all the diffraction peaks in the XRD pattern can be indexed to phase of CIS films deposited on SLG substrates annealed at 525 °C with chalcopyrite tetragonal structure, which are in good agreement with the standard values of the reported data (JCPDS No.40-1487) as the major phase and no secondary phase with a preferred orientation along (112) direction. The two weak peaks including (211), and (400) at ($2\theta = 35^o$ and 64^o) emerge here that distinguishes the chalcopyrite phase from the sphalerite phase. In addition, no peaks of other impurities were detected before annealing, indicating the high phase purity of CIS sample. From the figures one can observed that CIS films are polycrystalline structure where many peaks appeared.

A typical feature is that, in all the range of

Full Paper

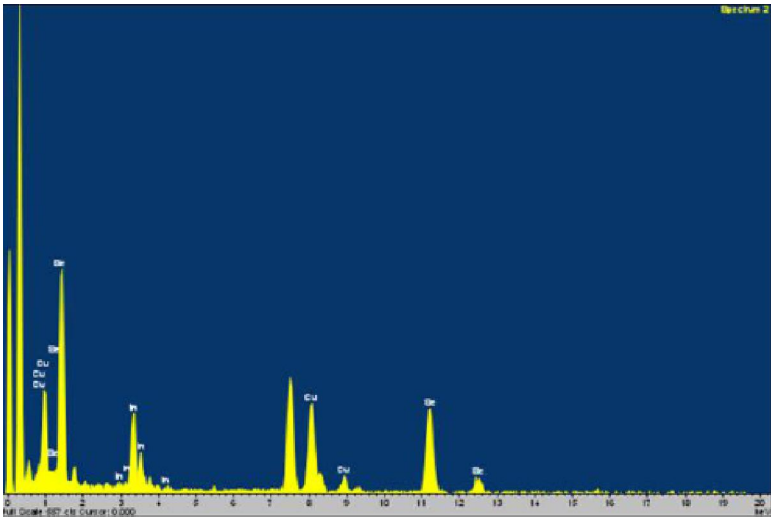

Figure 1 : EDS pattern of CIS DPP:Se

TABLE 1 : The Composition of $CuInSe_2$Nanoink Determined by EDS

Nanoink	Element	Weight %	Atomic %
CIS DPP:Se	Cu K	21.46	27.88
	In L	30.60	22.00
	Se L	47.94	50.12

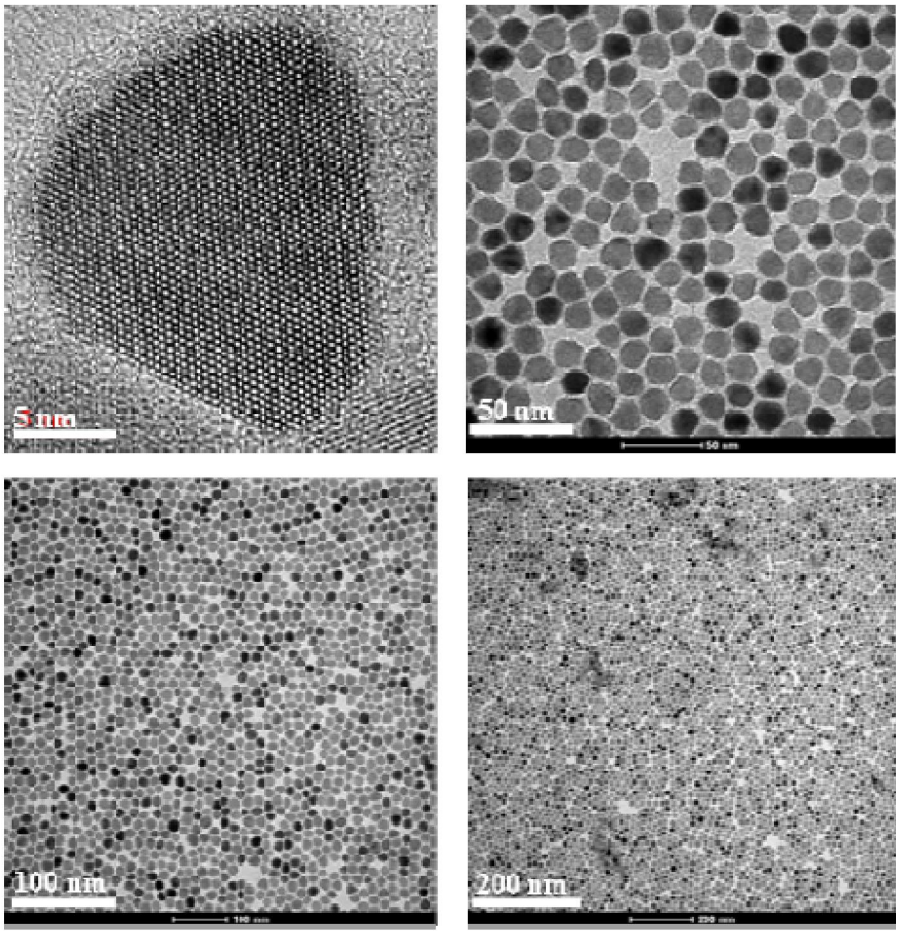

Figure 2 : TEM images of $CuInSe_2$ (CIS DPP:Se)

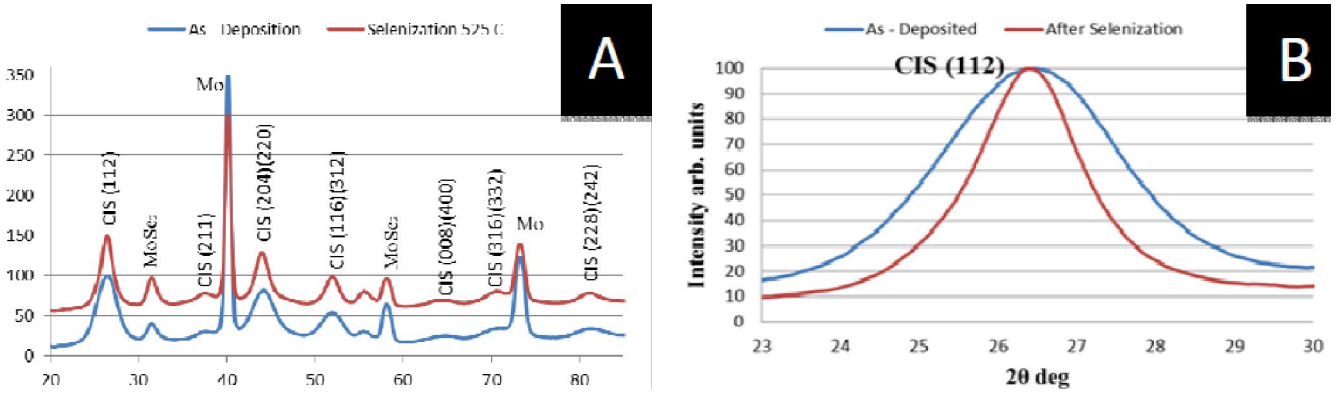

Figure 3 : XRD pattern of CIS DPP:Se :(A) as-deposited by spray-cast and after selenization, (B) comparison between $CuInSe_2$ peak (112) before and after selenization

compositions obtained, the samples exhibit a strong preferential orientation, The most intense peak is situated at approximately 26.50° which is belong to Miller indices. As could be seen from the XRD patterns, the three main diffraction peaks due to (112), (220) and (312) planes which are belong to (2θ = 26.58°, 44.18° and 52.34°) correspond to CIS.

In contrast, low intensity (112), (220) and (312) peaks were observed in the film before selenization. A prolonged selenization time could improve the intensity of diffraction peaks.

Figure 3B shows the (112) CIS diffraction peak is broad for films without annealing and baking, the (112) peak due to the CIS (2θ = 26.58°) become narrower after annealing at 525 °C for 1 h in Ar atmosphere., which corresponds to the presence of large particles as will show in SEM images.

The morphology of the CIS synthesized at 240 °C for 1 h shown in Figure 4. The product is mainly composed of a large amount of nanoparticles after annealing, and these CIS nanoparticles with irregular shapes were easily aggregated together.

It is clear from the figures that the film surface had relatively homogeneous polycrystalline grain structure. The surface morphology shows that the CIS composition before annealing (as deposition) has a small grain size and smooth surface but become nearly uniform, and dense surface with visible boundary after annealing. When annealing CIS composition, the grain size become much larger than the grain size in as-deposition composition.

The heat treatment at 525 °C for 4 h in Ar atmosphere is an important factor for producing bigger layer thickness which used for condense the homogeneity and improve the layer thickness of CIS thin film.

Small sintering observed for lower temperature deposition, but not for higher temperature. This could be related to the amount of solvent on the film during deposition. At higher temperatures, the film appears more uniform. Sintering occurs to a small extent, similar to the low temperature spray cast films.

The I-V response for the forward and reverse bias voltages of device architecture consisting of layers of glass/Mo/CIS/CdS/ZnO/ITO solar cell fabricated before and after selenization is shown in figures 5 for thicknesses of 150 nm and concentration 10 mg/ml of CIS DPP:Se nanocrystal layer deposited by spray – coating before and after selenization. It is clear that (PCE) increased after selenization from 0.631to 0.846 % .

Also it can be seen from these figure that for all samples, the forward current increases selenization. These may be due to the increase of carrier concentration which affected the energy band bending and thus result in a decreasing in depletion region width. In the reverse bias, the depletion region increases due to introduction of high barrier potential[17]. Reverse current increases with increasing bias voltage. The saturated current at reverse bias can be explained on the basis of the lack of tunneling mechanism[18].

One can notice that the illumination current increases with increasing of concentration x which is cause the increasing in the grain size and reducing of grain boundaries which lead to the increase of

Full Paper

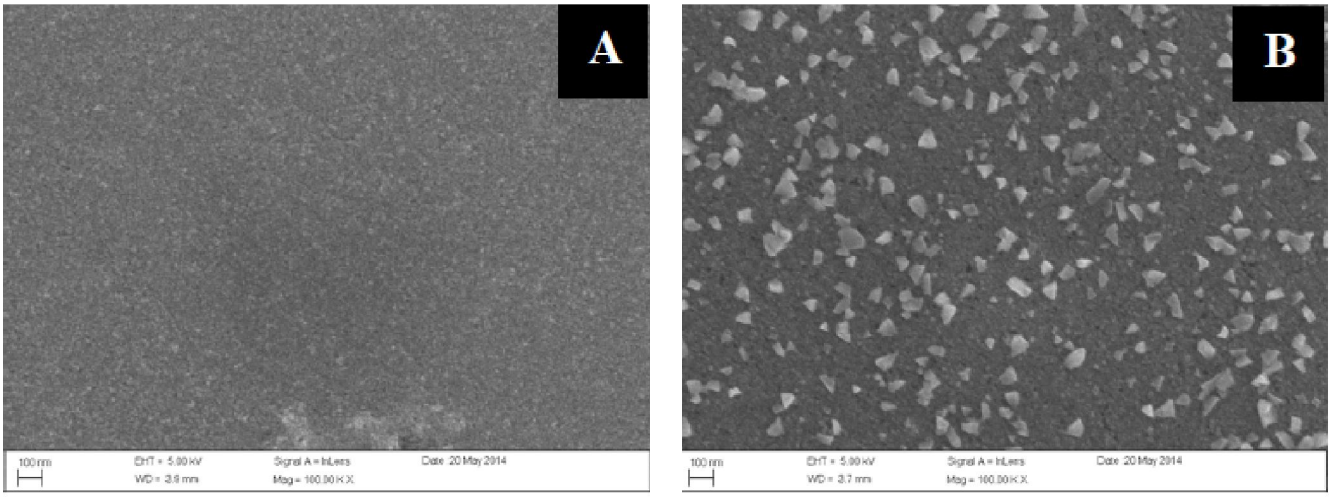

Figure 4 : SEM Images of CIS DPP:Se 150 nm layer deposited with 10 mg/ml by spray-casting: (A) before and (B) after selenization

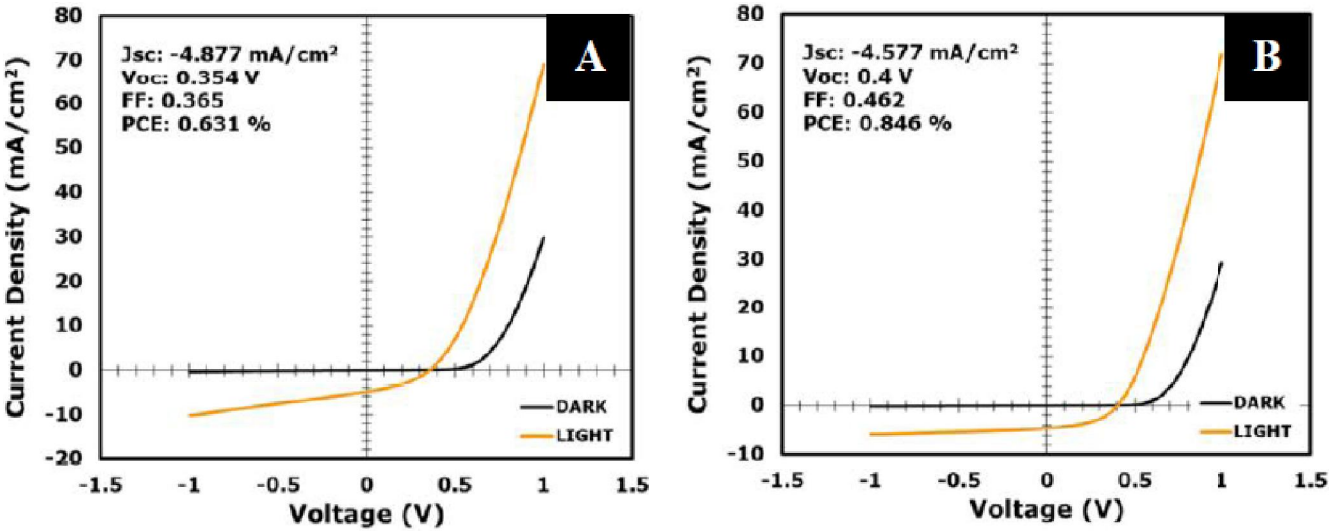

Figure 5 : I-V characteristics for Mo/CIS DPP:Se/CdS/ZnO/ITO heterojunction solar cell at thickness layer of 150 nm deposited by spray-coating: (A) as-deposited (B) after selenization

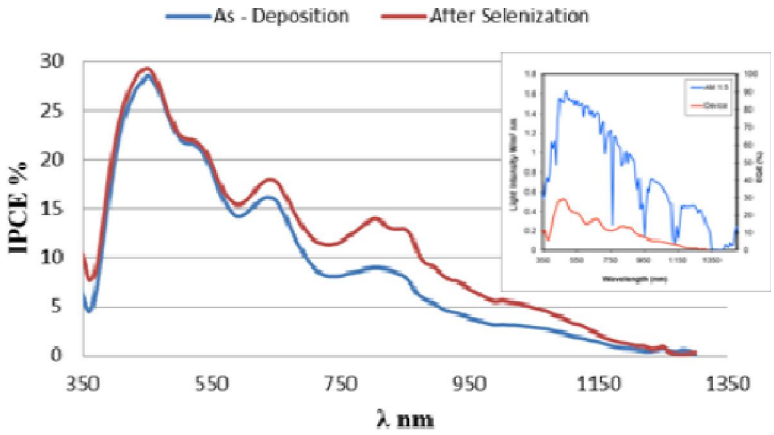

Figure 6 : IPCE measurements of Mo/CIS DPP:Se/CdS/ZnO/ITO devices

the mobility and increase the illumination current, the value of solar cell parameters.

Measurements of the incident photon-to-electron conversion efficiency (IPCE) provide additional

insight into how well the devices are performing and what the limiting factors are. Figure 6 The Mo/CIS DPP:Se/CdS/ZnO/ITO devices performed well under AM1.5 illumination, with a fill factor of 0.462 with a 350 nm.

The IPCE data is essentially an external quantum efficiency (at zero bias) that does not account for how much light is absorbed by the device. It is a measure of charge carriers extracted based on the number of photons that are illuminating the device. Efficient device performance of the devices is also enhanced by light reflection from the back contact. Especially, the films after selenization benefit from a "second pass" of light reflected off the back contact. This is evident in the IPCE measurements at longer wavelengths (600 nm to 1200 nm) where only a very small fraction of the incident light is absorbed by the thinner layers on the first pass. As the films get thicker, a large fraction of the incident photons are absorbed deeper in the nanocrystals layer and the resulting photogenerated carriers are unable to be efficiently extracted[19].

CONCLUSIONS

The device architecture consisting of layers of glass/Mo/CIS/CdS/ZnO/ITO solar cell fabricated before and after selenization for thicknesses of 150 nm and concentration 10 mg/ml of CIS DPP:Se nanocrystal layer deposited by spray – coating . It is clear that (PCE) increased after selenization from 0.631to 0.846 % .A prolonged selenization time could improve the intensity of diffraction peaks.the (112) peak due to the CIS become narrower after annealing at 525 °C for 1 h in Ar atmosphere.The surface morphology shows that the CIS composition before annealing (as deposition) has a small grain size and smooth surface but become nearly uniform, and dense surface with visible boundary after annealing. When annealing CIS composition, the grain size become much larger than the grain size in as-deposition composition.

REFERENCES

[1] S.B.Zhang, S.H.Wei, A.Zunger, H.Katayama-Yoshida; Phys.Rev.B, **57**, 9642 **(1998)**.

[2] Yoshimasa Tani, Kazunori Sato, Hiroshi Katayama-Yoshida; First-principles materials design of $CuInSe_2$-based high-efficiency photovoltaic solar cells, Physica B, **407**, 3056–3058 **(2012)**.

[3] K.Bindu, C.SudhaKartha, K.P.Vijayakumar, T.Abe, Y.Kashiwab; $CuInSe_2$ thin film preparation through a new selenisation process using chemical bath deposited selenium, Solar Energy Materials & Solar Cells, **79**, 67–79 **(2003)**.

[4] M.Ider, R.Pankajavalli, W.Zhuang, J.Y.Shen, T.J.Anderson; Thermochemistry of the Cu_2Se–In_2Se_3 system, Journal of Alloys and Compounds, **604**, 363–372 **(2014)**.

[5] 0.Tesson, M.Morsli, A.Bonnet, V.Jousseaume, L.Cattin, G.Masse; Electrical characterisation of CuInSe, Thin films for solar cells applications, Optical Materials, **9**, 511-515 **(1998)**.

[6] J.Szot, D.Haneman; Sol.Energy Mater., **11**, 289 **(1984)**.

[7] A.Parretta, M.L.Addonizio, A.Agati, M.Pellegrino, L.Quercia, F.Cardellini, J.Kessler, H.W.Schock; Jpn.J.Appl.Phys, .**32**, 80 **(1993)**.

[8] E.Tzvetkova, N.Stratieva, M.Ganchev, I.Tomov, K.Ivanova, K.Kochev; Thin Solid Films, **311**, 101 **(1997)**.

[9] S.Verma, N.Orbey, W.B.Robert, T.W.F.Russell; Prog.Photovolt.Res.Appl., **4**, 341 **(1996)**.

[10] J.Schmidt, H.H.Roscher, R.Labusch; Thin Solid Films, **251**, 116 **(1994)**.

[11] Vahid A.Akhavan, Brian W.Goodfellow, Matthew G.Panthani, Chet Steinhagen, Taylor B.Harvey, C.Jackson Stolle, Brian A.Korgel; Colloidal CIGS and CZTS nanocrystals: A precursor route to printed photovoltaics, Journal of Solid State Chemistry, **189**, 2–12 **(2012)**.

[12] C.Jackson Stolle, Taylor B.Harvey, Brian A.Korgel; Nanocrystal photovoltaics: A review of recent progress, Current Opinion in Chemical Engineering, **2**, 160–167 **(2013)**.

[13] V.A.Akhavan, B.W.Goodfellow, M.G.Panthani, D.K.Reid, D.J.Hellebusch, T.Adachi, B.A.Korgel; Energy Environ Sci., **3**, 1600 **(2010)**.

[14] V.A.Akhavan, M.G.Panthani, B.W.Goodfellow, D.K.Reid, B.A.Korgel; Opt Express, **18**, A411-A420 **(2010)**.

[15] C.J.Stolle, M.G.Panthani, T.B.Harvey, V.A.Akhavan, B.A.Korgel; ACS Appl Mater Interfaces, **4**, 2757-2761 **(2012)**.

[16] B.E.McCandless, W.N.Shafarman; US Patent, **6**,

Full Paper

537, 845 **(2003)**.

[17] B.D.Cullity; Elements of X-ray diffraction. Addison Wesley publishing co.Ltd.,London, **(1967)**.

[18] Hironori Katagiri, KotoeSaitoh, Tsukasa Washio, Hiroyuki Shinohara, Tomomi Kurumadani, ShinsukeMiyajima; Development of thin film solar cell based on Cu_2ZnSnS_4 thin films, Solar Energy Materials & Solar Cells, **65**, 141-148 **(2001)**.

[19] Vahid A.Akhavan; Photovoltaic Devices Based on $Cu(In_{1-x}Ga_x)Se_2$ Nanocrystal Inks, (Ph.D.Thesis) The University of Texas at Austin, Texas, **(2011)**.